

Received May 17, 2017, accepted May 30, 2017, date of publication July 12, 2017, date of current version July 24, 2017.

Digital Object Identifier 10.1109/ACCESS.2017.2711958

High-Q Substrate Integrated Waveguide Resonator Filter With Dielectric Loading

FAROUK GRINE¹, TAREK DJERAFI², (Member, IEEE), MOHAMED TAOUFIK BENHABILES¹, KE WU³, (Fellow, IEEE), AND MOHAMED LAHDI RIABI¹, (Member, IEEE)

¹University Frères Mentouri de Constantine, 25005 Constantine, Algeria

²Institut National de la Recherche Scientifique, Énergie Matériaux et Télécommunications, Montréal, QC H5A 1K6, Canada

³Poly-Grames Research Center, École Polytechnique de Montréal, Montréal, QC H3V 1A2, Canada

Corresponding author: Farouk Grine (faroukgrine@umc.edu.dz)

This work was supported by the Natural Sciences and Engineering Research Council of Canada.

ABSTRACT A planar cavity is proposed, designed, and implemented with a hybrid substrate integrated waveguide (SIW) and periodically drilled SIW (PDSIW) structure. Air holes are added to synthesize a lower effective permittivity. The periodicity can increase the stored energy and improve the quality factor. The optimal ratio between the two permittivities is investigated. The measured results show that the proposed resonator has an unloaded quality factor (Q_u) of 815, which is 53% higher than its standard SIW counterpart. To demonstrate the potential of the proposed PDSIW cavity, a third-order filter is designed and implemented through the proposed cavity, and it is then compared with filters of different orders. The new filter with a cavity shows performance enhancements in terms of both loss and bandwidth. The SIW resonator can be a promising element for use in the design of high-performance microwave filters and oscillators.

INDEX TERMS Air holes, cavity, filter, periodically drilled SIW, periodically loaded SIW, quality factor, substrate integrated waveguide (SIW).

I. INTRODUCTION

Microwave filters are essential components in all types of telecommunication systems. Trends in future applications of wireless technologies require the filters to be compact, exhibit a high selectivity with low insertion loss, and be lightweight [1]. To achieve these desired features simultaneously, considerable filter design efforts are required. Advanced small size resonators with high quality factors are also needed to overcome the problems that arise in this regard.

High-quality Q resonators are important for high performance filters, duplexers, and wireless communication circuits and systems. It is well known that a passive microstrip or microstrip-like resonator generally yields poor Q-related performance, which drastically limits its circuit applications [2]. Waveguide resonant cavities have been popular in the design of devices and circuits that require a high Q. They exhibit numerous advantages such as high-Q and high sensitivity [3]. However, their non-integrability in planar form prevents their use in low-cost systems.

The Substrate Integrated Waveguide (SIW) presents an attractive solution for the production of planar resonators due to its ease of fabrication and relatively high-Q factor. Therefore, it is of great importance in modern technology for many practical applications [4]. This technology is a good

compromise between the performance of classical waveguides and planar circuits, judging from the Q values and losses. For this reason, it raised a substantial amount of research in this field over the past several years. Various SIW passive microwave components and circuits have been successfully designed, demonstrated and deployed such as directional couplers [5], phase shifters [6], duplexers [7] and antennas [8]. The unloaded Q-factor of an SIW cavity can be determined by its losses, which depend primarily on the dielectric substrate dissipation, the finite metal conductivity, and the substrate radiation leakage through the gaps [9]. In fact, this is also closely related to the size, shape, and mode of the SIW cavity. The unloaded Q factor is usually limited in this case to a few hundreds [10]–[12]. The variation of the unloaded quality factor Q of a SIW resonator by changing the substrate parameters has been studied [12]. The results show that the energy stored in the resonator is related to the substrate thickness, the dielectric permittivity, and the loss tangent. A thicker substrate provides a lower loss, and for the same thickness, the SIW resonator provides significantly higher unloaded Q than did the microstrip resonator. The Q factor reaches a maximum of 580 with a substrate with $\epsilon_r = 2.2$, $\tan\delta = 0.0009$ and a 20 mil thickness.

In this paper, an alternative SIW resonator showing higher Q factor is proposed and developed. The idea is based on a periodic artificial modification of the main line material with permittivity ϵ_{r1} by drilling air vias in the substrate to reach a specific permittivity ϵ_{r2} . The parameters of periodicity and permittivity variation ratio are studied to achieve the optimal choice. The simulations and measurements are compared to demonstrate the overall performance of the proposed cavity. To estimate the potential of the proposed cavity, a SIW filter is implemented and compared with standard SIW filters.

II. DESIGN CONSIDERATION

Fig. 1 presents a basic structure of the proposed SIW cavity resonator. This figure shows the periodicity between the main line material with permittivity ϵ_{r1} and the periodic cell with permittivity ϵ_{r2} Fig. 1. (a). l_1 is the width of the cell and l_2 is the space between two adjacent unit cells. The permittivity of ϵ_{r2} is reached by drilling air vias in the substrate with permittivity ϵ_{r1} Fig. 1. (b). This figure also shows a unit cell of the periodic structure in Fig. 1. (c). Air vias with diameter d_i and inter-distance of p_i are used to synthesize the periodic cells. Two separate rows of metallic via slots are used to synthesize the rectangular cavity in a dielectric substrate.

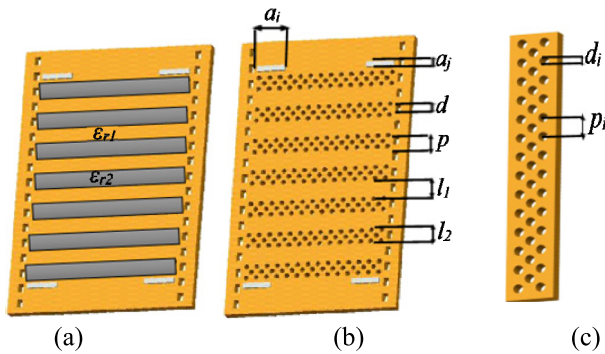


FIGURE 1. Proposed SIW cavity with periodic PSDIW (artificial synthesized dielectric): a) equivalent periodic dielectric, b) perspective view with periodic cavity, c) unit cell.

The loaded quality factor (Q_l) of a cavity is defined as

$$Q_l = \frac{f_0}{\Delta f_{3dB}} \tag{1}$$

Where f_0 is the resonant frequency and Δf is the -3 dB bandwidth. The external quality factor (Q_e) is defined as a function of S_{21} at resonant frequency f_0 and the loaded quality factor (Q_l) [13]

$$Q_e = \frac{Q_l}{10^{-IL/20}} \tag{2}$$

The unloaded Q-factor of an SIW cavity can be obtained through the equation

$$\frac{1}{Q_u} = \frac{1}{Q_l} - \frac{1}{Q_e} \tag{3}$$

In addition to dielectric and conductor losses, leakage loss may be present. However, the latter is nearly negligible with

the appropriate selection of the size and spacing of the metallic via-holes or posts [9]. The conductor loss includes the contributions of metallic via-hole or post arrays as well as that of bottom and top metal surfaces. Since the substrate thickness is much smaller than the equivalent width or length of SIW cavity resonators and transmission lines, the loss caused by the metallic via arrays is negligible in the total loss for most cases. Since the propagation characteristics of SIW are quite similar to those of a classical rectangular waveguide, closed-form attenuation constant formulas of an SIW transmission line can be used to model the proposed periodic structure in terms of loss and other related parameters. The resonant frequency is evaluated by using a rectangular waveguide model for SIW cavities.

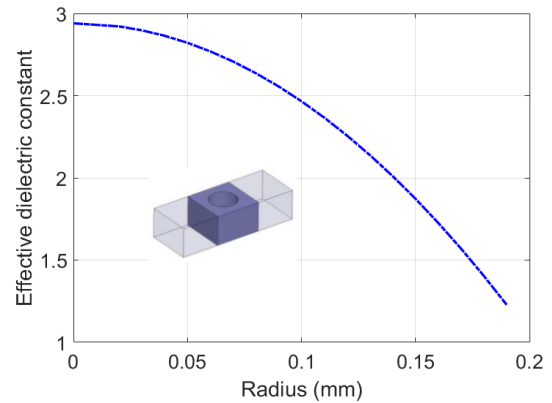


FIGURE 2. Effective dielectric constant of the substrate perforated with cylindrical air hole.

Air holes are used to decrease the substrate permittivity from ϵ_{r1} to ϵ_{r2} according to the air hole diameter d_i and periodicity p_i , as shown in Fig. 1. (c). The air-holes diameter in each part are determined based on the desired variation on the effective dielectric constant of the substrate perforated with cylindrical air-holes. For the periodic structure, the effective permittivity for a drilled air hole unit is calculated referring to [14]. The effective dielectric constant of the entire block can be calculated by $(\epsilon_{r1} - \Delta)$. This is achieved by introducing air holes to replace the lower relative permittivity sections, where a decrease in dielectric loss is expected due to the material removal. The value Δ is defined by dividing the difference between the permittivities of the main substrate and the air holes by the number of unit cells. Fig. 2 presents the results following a systematic study of the effective permittivity ϵ_{r2} in a periodically loaded SIW in which arrays of air holes are added along the waveguide ($\epsilon_{r1} = 2.94$) to synthesize a lower effective permittivity. Through this figure, the effective dielectric constant is a function of the radius of the air hole. The effective dielectric constant decreases as the radius of the air hole increases.

The waveguide dielectric loss can be calculated as an averaged function weighted by the drilled and undrilled surface in a periodic cell as follows:

$$\tan \delta = \frac{\tan \delta_0(\epsilon_{r2} - 1) * \epsilon_{r1}}{(\epsilon_{r1} - 1) * \epsilon_{r2}} \tag{4}$$

This assumption is valid in the case of total material removal ($\epsilon_{r2} = 1$) and without a hole ($\epsilon_{r2}=\epsilon_{r1}$) which corresponds to $\tan\delta = 0$ and $\tan\delta = \tan\delta_0$ respectively.

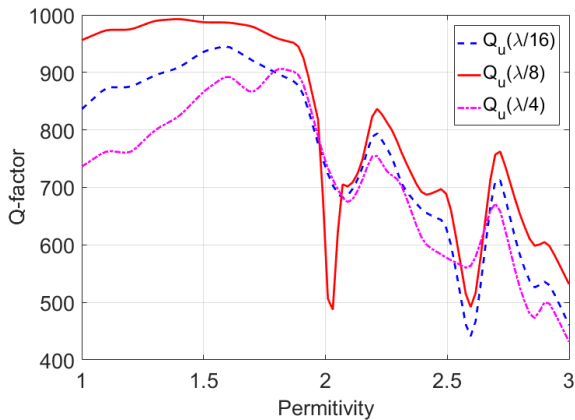


FIGURE 3. Simulated results of Q-factor of resonator cavity vs. permittivity.

To define the optimized parameters, a periodically dielectric slab of different length ($\lambda_g/4$, $\lambda_g/8$, $\lambda_g/16$) is analyzed [13]. For each case, the effect of variation of the slab’s effective permittivity on Q-factor is studied. The results are plotted in Fig. 3 for the structure in absence of radiation and metallic losses, which shows that the Q enhancement is not related to these two loss mechanism. The structure with perfect periodic blocks with permittivity ϵ_{r2} shown in fig. 1(a) is analyzed in this study. The substrate made of Rogers 6002 with a permittivity of 2.94 and a thickness of 0.508 mm is used in the main line. All structures are optimized at 10 GHz because the material characteristics are well-defined by the manufacturer at this frequency. The same Q_l factor ($\Delta f/f$) is maintained.

Fig. 3 suggests that the Q-factor increases as ϵ_{r2} decreases. Two spikes occur around 2.2 ($0.75\epsilon_{r1}$) and 2.7 ($0.9\epsilon_{r1}$). The use of $\lambda_g/8$ slab width shows a higher Q-factor compared to the cases of $\lambda_g/16$ and $\lambda_g/4$. In contrast, the introduction of air holes in lower relative dielectric permittivity material decreases the dielectric losses due to the removal of material. The reduction of dielectric loss involves a significantly improved Q-factor in the region of $\epsilon_{r2} < 1.8$. Fig. 4 shows the variation of the resonant frequency compared to the equivalent permittivity for the same cavity length. This figure shows that the resonant frequency decreases when the equivalent permittivity increases. This variation is linear with $\sqrt{\epsilon_{r2}}$.

The Q factor for a circuit is defined as the energy stored in the resonator and it is related to the power loss per oscillation period. Fig. 5 shows a comparison between the dispersion characteristics of the SIW waveguide and those of the periodic SIW/PDSIW waveguide with ϵ_{r2} of 2.2 for the fundamental mode calculated using Ansoft HFSS. To make the comparison meaningful, the parameters of the two waveguides are set to be identical. As shown in Fig. 5, the normalized phase velocity of the periodically loaded

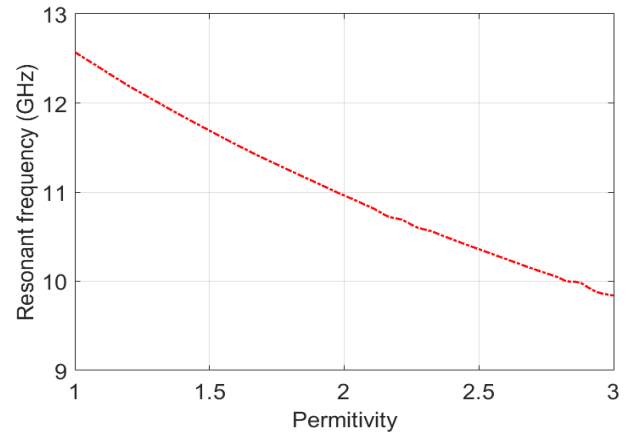


FIGURE 4. Simulated results of resonant frequencies vs. permittivity.

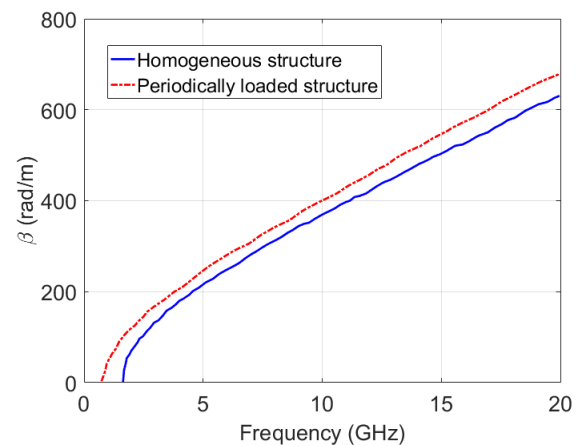


FIGURE 5. Simulated results of dispersion characteristics of SIW and PSIW.

waveguide is higher than that of the SIW waveguide, and the cut-off frequency is lower by approximately 7%. The cause of the Q factor enhancement is not only related to the loss reduction and the increase of the β , but is also related to the creation of a spatially separated electric and magnetic energy storage phenomenon that can be observed along slow-wave transmission lines [15]. The E and H field’s distributions at the resonant frequency of 10 GHz for the loaded and standard cavity are compared in Fig. 6, which shows more stored energy in the center of the loaded cavity. The distribution is less sinusoidal in this case showing that the stored energy has increased. The variation of the media acts the same way as a shunt capacitive reactance which stores additional energy. The resonator model is composed of two inductances and periodic capacitance. The iris places a shunt inductive reactance across the waveguide that is directly proportional to the size of the opening. The reactance is directly proportional to the permittivity ratio.

The unloaded Q-factor is also determined by the resonator conductor and dielectric losses. To estimate this factor, the different losses mechanisms effects are estimated. The slab is substituted by PDSIW as illustrated in Fig. 1(c); the radiation effect by the air holes in the drilled SIW has been studied.

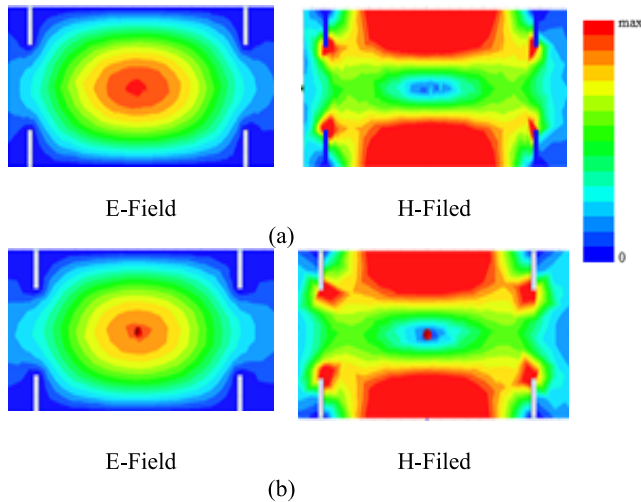


FIGURE 6. E and H field's distributions in the resonator: (a) With dielectric loading, (b) Without dielectric loading.

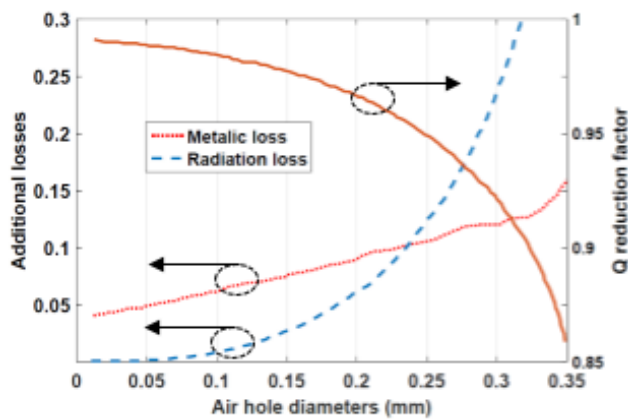


FIGURE 7. Simulated Q, reduction factor, radiation loss and metallic loss in function of via diameter.

Fig. 7 presents the results of this study and concludes that radiation losses are not significant with air hole diameters of 0.05 mm, which corresponds to the first Q-factor max spike ($\epsilon_{r2}=2.7$). The radiation loss causes a reduction of Q-factor by approximately 15% with air-hole diameter of 0.35 mm, which corresponds to ϵ_{r2} of 1.5. Fig. 7 also plots the metallic loss of a transmission line in which the circuit material is assumed to be copper with a conductivity value of 2.4×10^7 S/m at 10 GHz. It is shown in Fig. 7 that the total additional loss to the cavity is approximately 0.13 dB at $\epsilon_{r2} = 2.2$ which is equivalent to a 3% drop in Q-factor and 0.05 dB at $\epsilon_{r2} = 2.7$ corresponding to a 1% drop. The drop in the case of a slab permittivity equivalent to 1.8 is approximately 10% and decreases dramatically afterward.

An unloaded Q factor of 815 is achievable with the proposed method. The effect of this enhancement on the filter performance should be studied further.

III. FILTER STRUCTURE

Fig. 8 shows the horizontal cross section of the proposed filter with three-cavity resonators. In this figure, separate

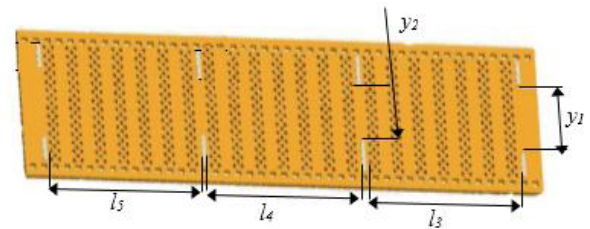


FIGURE 8. Proposed SIW filter with periodic PDSIW (artificial Dielectric).

rows of metallic via slots are used to synthesize the three rectangular cavities. y_1 and y_2 are the distances between two facing metalized via slots for the first and second cavities, respectively, which defines the iris. l_3 , l_4 and l_5 are the lengths of the three cavity resonators.

The insertion loss IL within the bandpass filter depends on three principal factors: the unloaded quality factor of resonators Q_u , fractional bandwidth $\Delta f/f_0$ and the filter order N . Depending on these factors, we can evaluate the minimum insertion loss within the bandpass at frequency f_0 as follows [16]:

$$IL(f_0) \approx 4.343 \frac{N}{Q_u \frac{\Delta f}{f_0}} \quad (5)$$

According to relation (5), to improve the selectivity of the filter, we need to increase the number of resonators involved N . However, this leads to a rise in the insertion loss at the same time, which leads us to increase the unloaded quality factors to reduce the insertion loss. As demonstrated in the previous section, the insertion losses IL can be minimized by introducing a periodic artificial dielectric slab in the cavity, which we used to design the filter.

The optimal dimensions of the simulated filter of order 3 with dielectric loading (according to the parameters annotation in Fig. 8) are: $y_1 = 7.344$ mm, $y_2 = 5.05$ mm, $l_3 = l_5 = 18.1216$ mm, $l_4 = 19.1984$ mm.

To demonstrate the effectiveness of this design, the insertions losses of filters without dielectric loading of orders 3 and 4 and of filter with dielectric loading of order 4 are compared in Fig. 9. This figure also shows the comparison between the return losses. For the filter with three-cavity SIW without dielectric loading, the center frequency is 10.05 GHz, bandwidth $BW = 900$ MHz (8.95%), the minimum insertion loss is less than 0.66 dB. For the filter with four-cavity SIW without dielectric loading, the center frequency is 10.03 GHz, and the bandwidth $BW = 1.443$ GHz (14.8%). In this case, the bandwidth is increased by 5.85% compared with the previous filter, and the minimum insertion loss is less than 0.45 dB. For the filter with four-cavity SIW with dielectric loading, the center frequency is 10.02 GHz, and the bandwidth $BW = 1.553$ GHz (15.5%). For this filter as well, the bandwidth is increased by 0.7% compared with the same filter without dielectric loading, while the minimum insertion loss is less than 0.35 dB. The high Q-factor allows a wider bandwidth with lower insertion loss.

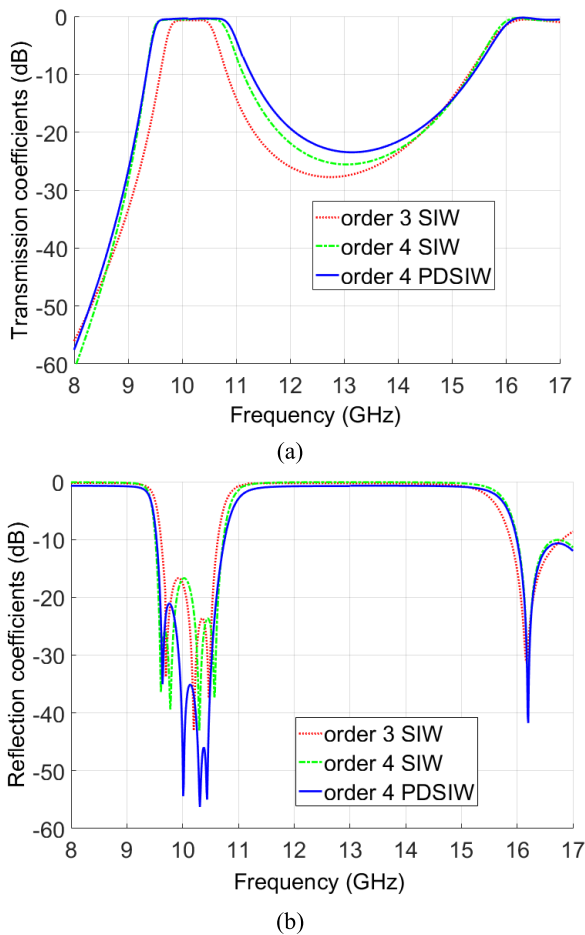


FIGURE 9. S-parameters of the three filters: (a) transmission coefficients, (b) reflection coefficients

IV. SIMULATED AND MEASURED RESULTS

Following a parametric optimization through Ansoft HFSS, a cavity is designed and fabricated to validate the proposed concept and is compared to the simulated results. The optimized dimensions of the fabricated cavity shown in Fig. 10 are as follows: $l_1 = 1.25$ mm, $l_2 = 1.25$ mm, $w = 10.067$ mm, $h = 0.708$ mm, $a_i = 2.391$ mm, $a_j = 0.354$ mm, $d = 0.707$ mm, $p = 0.352$ mm, $d_i = 0.3934$ mm, $p_i = 0.352$ mm.

Fig. 11 shows the simulated and measured S parameters of the proposed resonator. A good agreement is observed between the simulated and experimental values. The resonance frequency of the SIW cavity is shifted to 9.97 GHz with respect to the simulated value of 10 GHz and the measured insertion loss is higher than the simulated counterpart. The measured unloaded Q-factor of the cavity is higher than 800, as expected.

The measured results show a loaded Q factor of 60 and unloaded Q factor of 815 with the dielectric loaded SIW resonator. It can be observed that in Table 1, the unloaded Q-factor of the proposed SIW resonator is greatly improved compared with same cavity without dielectric loading (with

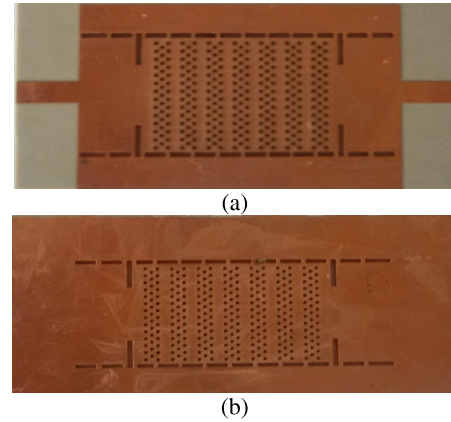


FIGURE 10. Photograph of the proposed SIW cavity. (a): front side; (b): back side.

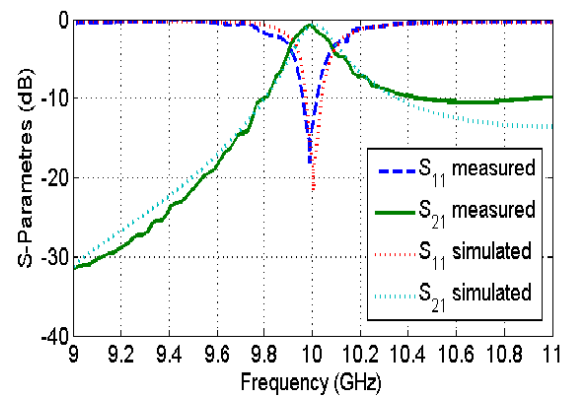


FIGURE 11. S-parameter of the proposed cavity.

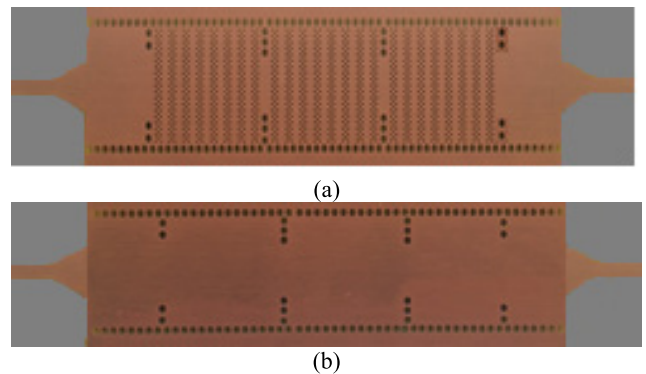


FIGURE 12. Photograph of the proposed SIW filter. (a): front side; (b): back side.

the same loaded Q factor of 60), with an increase in size of approximately 5%. Compared with the same type of SIW cavities reported in previous studies over the same frequency range, the Q-factor of the proposed SIW resonator is greatly improved. However, the Q-factor is still higher in the standard rectangular resonator in which the height is larger.

The proposed filter with three cavities is designed using the same substrate of resonator cavity. The optimized dimensions of the fabricated filter shown in Fig. 12, were presented in the

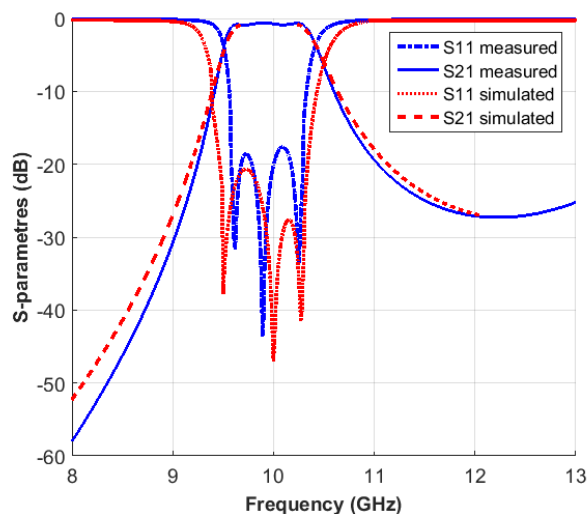


FIGURE 13. S-parameter of the proposed filter with three poles.

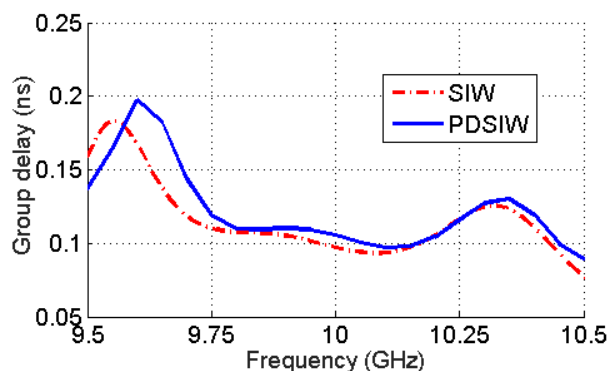


FIGURE 14. Simulated group delay of S21.

TABLE 1. Comparison of different SIW cavity resonators.

	Freq (GHz)	Substrate ($\epsilon_r/tg\delta/h$ (mm))	QU	Length (mm)	Width (mm)
This work	10	2.94/0.0023/0.508	815	25.7356	10.0678
Without	10	2.94/0.0023/0.508	500	24.298	10.13
[10]	10	2.33/0.0012/0.508	540	-	-
[11]	10.8	3.55/0.0023/1.524	373.3	-	-

simulation section. The simulated and measured responses of the proposed filter are shown in Fig. 13. A good agreement is observed between the simulated and experimental values.

As shown in Fig. 13, the center frequency for the simulated results is 9.98 GHz, with a difference of approximately 0.01 for the measured results (9.99 GHz). The bandwidth $BW = 1.1\text{GHz}$ for the simulation and 0.9 GHz for the measured results, and the minimum insertion loss is less than 0.46 dB and 0.48 dB for the simulated and measured results respectively.

Figure 14, presents the simulated results of the group delay of S21 for the two structures (standard SIW, PDSIW).

The first structure attains a maximum group delay of 0.19 ns, and the minimum group delay of 0.08 ns. About the proposed design (PDSIW) the maximum group delay is less than 0.2 ns and the minimum is 0.09 ns, throughout the passband. In all this duration, the proposed design present a phase behavior of the signal remains linear, which is very smooth for the microwave filter. Comparison of the group delay of S21 with other types of filters is not available here because most of the filters presented in references haven't been reported.

V. CONCLUSION

In this paper, a synthesized resonator based on a hybrid structure of substrate integrated waveguide and periodically drilled substrate integrated waveguide is developed and used to implement a filter. The operating principle and design procedure have been discussed. The resonator and filter have been designed, fabricated and measured to verify the proposed scheme. The periodicity is able to increase the stored energy, and it has been shown that the Q-factor can be increased. An optimal ratio of 0.9 between the main waveguide and the artificially synthesized substrates permittivity with an optimal periodicity of $\lambda/8$ are defined. These criteria increase the Q_u factor by approximately 53% with only a 5% increase in size. Materials with a larger thickness and a lower loss can also be used to increase the Q-factor. A filter is built to estimate the enhancement in the performance using the proposed cavities. The results show excellent performance in terms of bandwidth and loss. The proposed technique is promising and presents a competitive candidate for the development of RF/microwave circuits and systems.

REFERENCES

- [1] C. Tomassoni, S. Bastioli, and R. V. Snyder, "Propagating waveguide filters using dielectric resonators," *IEEE Trans. Microw. Theory Techn.*, vol. 63, no. 12, pp. 4366–4375, Dec. 2015.
- [2] A. Gopinath, "Maximum Q-factor of microstrip resonators," *IEEE Trans. Microw. Theory Techn.*, vol. MTT-29, no. 2, pp. 128–131, Feb. 1981.
- [3] E. Pucci, A. U. Zaman, E. Rajo-Iglesias, P.-S. Kildal, and A. Kishk, "Study of Q-factors of ridge and groove gap waveguide resonators," *IET Microw., Antennas Propag.*, vol. 7, no. 11, pp. 900–908, Aug. 2013.
- [4] Q.-L. Yang, Y.-L. Ban, K. Kang, C.-Y.-D. Sim, and G. Wu, "SIW multi-beam array for 5G mobile devices," *IEEE Access*, vol. 4, pp. 2788–2796, Jun. 2016.
- [5] A. Doghri, T. Djerafi, A. Ghiotto, and K. Wu, "Substrate integrated waveguide directional couplers for compact three-dimensional integrated circuits," *IEEE Trans. Microw. Theory Techn.*, vol. 63, no. 1, pp. 209–221, Jan. 2015.
- [6] T. Djerafi, K. Wu, and S. O. Tatu, "Substrate-integrated waveguide phase shifter with rod-loaded artificial dielectric slab," *Electron. Lett.*, vol. 51, no. 9, pp. 707–709, Apr. 2015.
- [7] Z. Kordiboroujeni and J. Bornemann, "K-band backward diplexer in substrate integrated waveguide technology," *Electron. Lett.*, vol. 51, no. 18, pp. 1428–1429, Aug. 2015.
- [8] Y. Cai, Y. Zhang, Z. Qian, W. Cao, and S. Shi, "Compact wideband dual circularly polarized substrate integrated waveguide horn antenna," *IEEE Trans. Antennas Propag.*, vol. 64, no. 7, pp. 3184–3189, Jul. 2016.
- [9] M. Bozzi, L. Perregini, and K. Wu, "Modeling of conductor, dielectric, and radiation losses in substrate integrated waveguide by the boundary integral-resonant mode expansion method," *IEEE Trans. Microw. Theory Techn.*, vol. 56, no. 12, pp. 3153–3161, Dec. 2008.
- [10] Y. Cassivi, L. Perregini, K. Wu, and G. Conciauro, "Low-cost and high-Q millimeter-wave resonator using substrate integrated waveguide technique," in *Proc. Eur. Microw. Conf.*, vol. 2. Milan, Italy, Sep. 2002, pp. 1–4.

- [11] H. E. Matbouly, N. Boubekeur, and F. Domingue, "A novel chipless identification tag based on a substrate integrated cavity resonator," *IEEE Microw. Wireless Compon. Lett.*, vol. 23, no. 1, pp. 52–54, Jan. 2013.
- [12] A. A. Khan, M. K. Mandal, and S. Sanyal, "Unloaded quality factor of a substrate integrated waveguide resonator and its variation with the substrate parameters," in *Proc. Int. Conf. Microw. Photon. (ICMAP)*, Dec. 2013, pp. 1–4.
- [13] J. Papapolymerou, J.-C. Cheng, J. East, and L. P. B. Katehi, "A micromachined high- Q X-band resonator," *IEEE Microw. Guided Wave Lett.*, vol. 7, no. 6, pp. 168–170, Jun. 1997.
- [14] R. Isidro, A. Coves, M. A. Sánchez-Soriano, G. Torregrosa, E. Bronchalo, and M. Bozzi, "Systematic study of the effective permittivity in a periodically drilled siw waveguide," in *Proc. 34th Progr. Electromagn. Res. Symp. (PIERS)*, Stockholm, Sweden, Aug. 2013, pp. 1870–1874.
- [15] K. Wu, "Slow wave structures," in *Wiley's Encyclopedia of Electrical and Electronics Engineering* (on the Microwave Theory and Techniques), vol. 19, J. G. Webster, Ed. Hoboken, NJ, USA: Wiley, 1999, pp. 366–381.
- [16] V. Turgaliev, D. Kholodnyak, J. Mueller, and M. A. Hein, "Small-size low-loss bandpass filters on substrate-integrated waveguide capacitively loaded cavities embedded in low temperature co-fired ceramics," *J. Ceram. Sci. Technol.*, vol. 6, no. 4, pp. 305–314, 2015.



of the IEEE Microwave Theory and Techniques Society.

FAROUK GRINE received the Licentiate and master's degrees in electronic from the University Frères Mentouri de Constantine, Algeria, in 2009 and 2011, respectively, where he is currently pursuing the Ph.D. degree with the Laboratory of Electromagnetism and Telecommunication. His current research interests include the telecommunication antennas, beam forming network, and RF/millimeter-wave/terahertz components, and systems design. He is a Student Member



from 2014 to 2015.

TAREK DJERAFI (M'12) received the B.Sc. degree from the Institut d'Aeronautique de Blida, Blida, Algeria, in 1998, and the M.A.Sc. and Ph.D. (Hons.) degrees in electrical engineering from the École Polytechnique de Montréal, Montreal, QC, Canada, in 2005 and 2011, respectively. He was an EMC Expert with SCP SCIENCE, Montreal, from 2010 to 2011, and a Post-Doctoral Fellow with INRS-EMT, Montreal, from 2012 to 2014, and the École Polytechnique de Montreal

from 2014 to 2015. He was a Research Associate with the Poly-Grames Research Center, Montreal, from 2015 to 2016. He is currently an Assistant Professor with the Institut National de Recherche Scientifique, Énergie Matériaux et Télécommunications, Montreal. His current research interests include the telecommunication antennas, beam forming network, and RF/millimeter-wave/terahertz components, and systems design.



MOHAMED TAOUFIK BENHABILES received the Ingénieur Civil Electricien degree from the Université Catholique de Louvain, Belgium, in 1982, and the Magister and Ph.D. degrees in electronics from the University Frères Mentouri de Constantine, Algeria, in 1995 and 2003, respectively, where he is currently a Senior Lecturer. His main research area is the numerical modeling of passive microwave devices.



KE WU (M'87–SM'92–F'01) received the B.Sc. degree (Hons.) in radio engineering from Southeast University, Nanjing, China, in 1982, the D.E.A. degree (Hons.) in optics, optoelectronics, and microwave engineering from the Institut National Polytechnique de Grenoble, Grenoble, France, in 1984, and the Ph.D. degree (Hons.) in optics, optoelectronics, and microwave engineering from the University of Grenoble, Grenoble, in 1987. He was the Founding Director of the Center for Radiofrequency Electronics Research of Quebec (Regroupement stratégique de FRQNT) and the Tier-I Canada Research Chair in RF and millimeter-wave engineering. He also held guest, visiting, and honorary professorships with many universities around the world. He has been the Director of the Poly-Grames Research Center, Montreal, QC, Canada. He is currently a Professor of Electrical Engineering and the NSERC-Huawei Industrial Research Chair in future wireless technologies with the Polytechnique Montréal, University of Montreal, Montreal. He has authored or co-authored over 1100 referred papers and a number of books/book chapters. He holds over 40 patents. His current research interests include substrate integrated circuits, antenna arrays, advanced computer-aided design and modeling techniques, nonlinear wireless technologies, wireless power transmission and harvesting, and development of RF and millimeter-wave transceivers and sensors for wireless systems and biomedical applications, and also the modeling and design of microwave and terahertz photonic circuits and systems.

Dr. Wu is a member of the Electromagnetics Academy, Sigma Xi, and URSI. He was an elected IEEE Microwave Theory and Techniques Society (MTT-S) Administrative Committee (AdCom) Member from 2006 to 2015. He is the Inaugural Three-Year Representative of North America as a member of the European Microwave Association General Assembly. He is a fellow of the Canadian Academy of Engineering and the Royal Society of Canada (The Canadian Academy of the Sciences and Humanities). He was a recipient of many awards and prizes, including the first IEEE MTT-S Outstanding Young Engineer Award, the 2004 Fessenden Medal of the IEEE Canada, the 2009 Thomas W. Eadie Medal of the Royal Society of Canada, the Queen Elizabeth II Diamond Jubilee Medal in 2013, the 2013 FCCP Education Foundation Award of Merit, the 2014 IEEE MTT-S Microwave Application Award, the 2014 Marie-Victorin Prize (Prix du Québec—the highest distinction of Québec in the natural sciences and engineering), the 2015 Prix d'Excellence en Recherche et Innovation of Polytechnique Montréal, and the 2015 IEEE Montreal Section Gold Medal of Achievement. He has held key positions in and has served on various panels and international committees, including the Chair of Technical Program Committees, International Steering Committees, and International Conferences/Symposia. In particular, he was the General Chair of the 2012 IEEE MTT-S International Microwave Symposium.. He was the Chair of the joint IEEE Chapters of MTT-S/AP-S/LEOS, Montreal. He has served as the Chair of the IEEE MTT-S Transnational Committee, a Member of the Geographic Activities Committee and the Technical Coordinating Committee among many other AdCom functions. He was an IEEE MTT-S Distinguished Microwave Lecturer during 2009–2011. He is currently the Chair of the newly restructured IEEE MTT-S Montreal Chapter and the 2016 IEEE MTT-S President. He has served on the Editorial/Review Boards of many technical journals, transactions, proceedings and letters, and scientific encyclopedia, including as an Editor or a Guest Editor



MOHAMED LAHDI RIABI received the Ingénieur en Electronique degree from Ecole Polytechnique, Algeria, in 1979, and the Ph.D. degree in microwave from the Université de Toulouse, France, in 1992. He is currently a Teaching Professor with the University Frères Mentouri de Constantine, Algeria. He is the Chairman of the Laboratory of Electromagnetism and Telecommunication, University Frères Mentouri. His research interests are microwave passive devices.

...